IJSGS FUGUSAU VOL. 11(3)

ISSNp: 2488-9229; ISSNe: <u>3027-1118</u>

WEBSITE: https://fugus-ijsgs.com.ng

INTERNATIONAL JOURNAL OF SCIENCE FOR GLOBAL SUSTAINABILITY

(A PUBLICATION OF FACULTY OF SCIENCE, FEDERAL UNIVERSITY GUSAU, NIGERIA)

Study of Phytochemicals and FTIR Spectra of Fractions from *Datura Metel* Linn (Non-Sedative Analgesic Plant)

¹Musa Runde, ²Mohammed Hassan Shagal, ²Douglass Wilson

¹Department of Chemistry, National Open University of Nigeria ²Department of Applied Chemistry, Modibbo Adama University, Yola

Corresponding Author's Email: rmusa@noun.edu.ng

Received on: August, 2025 Revised and Accepted on: September, 2025 Published on: October, 2025

ABSTRACT

This study investigated *Datura metel Linn*. to identify phytochemicals with non-sedative analgesic potential, offering an alternative to conventional sedative drugs. Bioactive compounds were isolated from leaves via sequential solvent extraction (acetone, chloroform, water) and fractionated by column chromatography, yielding primary (GH1-GH7) and secondary fractions. Phytochemical screening confirmed alkaloids, flavonoids, saponins, and steroids. Fourier Transform Infrared (FTIR) spectroscopy revealed diverse functional groups. Early fractions (e.g., GH1F1, GH2F2) showed signatures of aromatic carboxylic acids, with patterns consistent with para-substituted benzoic acid derivatives like 4-aminobenzoic acid (PABA), indicated by carbonyl stretches (1708-1735 cm⁻¹) and aromatic vibrations. Some fractions indicated inorganic ions. Later fractions (GH3F3-GH7F2B) exhibited classical plant extract profiles with broad O-H stretches (phenols, carbohydrates), aliphatic C-H stretches (lipids), ester carbonyl bands (1727-1731 cm⁻¹), and aromatic C=C bends (1515-1567 cm⁻¹), confirming a rich mixture of flavonoids, tannins, and phenolic compounds. The successful fractionation isolated a wide spectrum of phytochemicals. The dominance of functional groups linked to phenolic acids and flavonoids, known for anti-inflammatory and non-sedative analgesic activities, underscores the plant's therapeutic potential. The phytochemical profile of Datura metel L. reveals bioactive compounds supporting its traditional use. The collective anti-inflammatory action of flavonoids, tannins, and saponins suggests a viable basis for non-sedative analgesia. Identifying these distinct chemical signatures provides a foundation for future research, recommending advanced structural elucidation via NMR and mass spectrometry, followed by biosimulation and biological assays to validate pharmacological activity.

Keywords: Analgesic, Anti-inflammatory, Non-sedative, Phytochemicals, Isolation.

1.0 INTRODUCTION

Pain remains one of the most common clinical symptoms and continues to drive the search for effective and safe analgesic agents (Okonkwo et al., 2022). Conventional synthetic analgesics, such as opioids and non-steroidal anti-inflammatory drugs (NSAIDs), are effective but are often associated with undesirable side effects including sedation, dependence, gastrointestinal toxicity, and tolerance (Rang & Dale, 1997). As a result, medicinal plants are increasingly studied for their potential to provide non-sedative analgesic relief (Ekiert et al., 2021). Traditional medicine has historically used numerous plants for pain relief. According to the World Health Organization (WHO, 2004), up to 80% of the world's population relies on herbal medicines for primary healthcare. The scientific validation of these practices requires careful phytochemical analysis, isolation of bioactive constituents, and characterization using advanced techniques such as Fourier Transform Infrared (FTIR) spectroscopy (Ahmad et al., 2023).

Phytochemicals are plant-derived bioactive compounds that include alkaloids, flavonoids, tannins, glycosides,

saponins, and terpenoids, and their pharmacological properties often determine the therapeutic value of plants (Trease & Evans, 1996). In Datura metel, alkaloids such as scopolamine, hyoscine, and atropine are abundant, acting on muscarinic acetylcholine receptors and frequently inducing central nervous system (CNS) depression; while scopolamine is associated with sedation and delirium, its analgesic potential remains debated (Farha et al. 2020). Flavonoids, another major group, are polyphenolic compounds with antioxidant, anti-inflammatory, and analgesic activities, which partly function by inhibiting cyclooxygenase (COX) enzymes and suppressing prostaglandin synthesis (Trease & Evans, 1996; Mutha et al., 2021). Tannins contribute antimicrobial and anti-inflammatory properties, while cardiac glycosides primarily affect cardiovascular function but can indirectly influence nociceptive mechanisms (Farha et al, 2020). Comparatively, other as Ocimum gratissimum and Zingiber plants officinale demonstrate stronger analgesic responses, effects largely attributed to the presence of flavonoids and terpenes (Abubakar and Haque, 2020; WHO, 2004; Toma et al., 2020).



The phytochemical screening of Datura metel revealed the presence of important pharmacological bioactive substances as well as medicinal and nutritional potentials in the leaves (Anitha Muthusamy et al., 2014). The antibacterial activities of the studied plant extracts were comparable to the reference antibiotic (positive control) used. Therefore, this study offers a scientific basis for the use of the plant extracts for the treatment of infections that could be caused by the strains of the test bacterial organisms (Anitha Muthusamy et al., 2014). It is thus suggested that more studies on concentrations of active ingredients, antinutritional factors and toxicity level be carried out. From the plant saponins, flavonoids, phenols, alkaloids, glycosides, and steroids were identified in aqueous extract (Akharaiyi, 2011). In the chloroform extract steroids, flavonoids, triterpenoids were absent and tannins was absent in the acetone extract (Njeru et al, 2020). Current study agrees the above literature except tanins which was not recorded in any of the extracts used.

Analgesic screening of D. metel seed extracts in rats demonstrated no significant antinociceptive activity in both acetic acid-induced writhing and radiant heat tail-flick tests (Farha et al, 2020). Pentazocin produced strong analgesia, while D. metel extracts failed to match even the negative control at certain doses. Sedative effects such as reduced appetite and lethargy were observed, suggesting CNS depression (Rang & Dale, 1997).

While users reported pain relief from D. metel, experimental results show sedation without true analgesia (Farha et al, 2020). This discrepancy may be due to subjective relief via CNS depression, variation in alkaloid content, or synergistic effects in multi-herb preparations (Patel & Soni, 2022). Non-sedative analgesics are more likely to be found in flavonoid- or terpene-rich fractions (Okonkwo et al., 2022).

1.1 Objective

Using sequential solvent extraction (acetone, chloroform, and water) and column chromatography, the study aims to separate and fractionate bioactive compounds from Datura metel Linn. leaves. Additionally, the aqueous leaf extract will undergo qualitative phytochemical screening to detect the presence of important secondary metabolites, including alkaloids, flavonoids, tannins, saponins, and steroids. In addition, the study intends to use Fourier Transform Infrared (FTIR) spectroscopy to characterize the functional groups found in the isolated primary and secondary fractions (GH1 to GH7), analyze and interpret the resulting spectra to identify particular chemical signatures, such as those of aromatic carboxylic

WEBSITE: https://fugus-ijsgs.com.ng

acids, esters, phenols, and possible inorganic ions, and correlate them with known phytochemical classes. Lastly, the study aims to assess Datura metel's phytochemical profile in light of its traditional use and talk about the compounds' potential for therapeutic use, especially flavonoids and phenolic acids, which have a non-sedative analgesic impact.

2.0. MATERIALS AND METHODS 2.1 Methods

2.1.1 Collection and Preparation of Pant Materials

The fresh and disease-free leaves of Datura *metel* were collected from agricultural form house at vennandhur, Namakkal district. The fresh leaves were washed with distilled water, shade dried and the leaves were completely powdered by the use of grinder (Kumar et al., 2021).

2.1.2. Preparation of Etracts

air dried and powdered materials 1000mgforeach1000mgforeach were extracted with 10ml of acetone, chloroform and water by using soxhelet apparatus for 72 hours at a temperature not exceeding the boiling point (Sharma et al., 2020). The powdered sample was added to sohxlet apparatus and solvent is added to it in 1:5 ratios. The solvent system used in an increasing order as polarity acetone-Chloroform-Distilledwateracetone-Ch loroform-Distilledwater. Then the extract was collected from sohxlet apparatus and kept in room temperature for air-drying. The residues were collected, weighed and stored in 4°C for future use (Do et al, 2021).

2.1.3. Column Chromatography and Fractionation

A slurry of silica gel was prepared by mixing 50 g of silica gel (60–120 mesh, analytical grade) with hexane as the mobile phase. The slurry was carefully packed into a glass column to achieve a uniform stationary phase bed, following standard column chromatography protocols (Egbuna et al, 2019; Cruz, 2023).

The crude sample was dissolved in dimethyl ether and subsequently introduced onto the top of the packed column. Elution was carried out under gravity, and the fractionation process was allowed to run continuously for one week. Fractions were collected sequentially and labeled as GH1, GH2, GH3, GH4, GH5, GH6, and GH7. Each of these fractions was subjected to further fractionation using the same chromatographic procedure. For every primary fraction, three secondary fractions were obtained and tagged accordingly. For instance, GH1 yielded GH1F1, GH1F2, and GH1F3, while GH2 yielded GH2F1, GH2F2, and GH2F3, and so forth.

2.1.4. Extraction and Isolation



25 grams of sample was transfer into a timble and inserted into a Soxhlet extractor, and 100 mls of distilled water was added into the flask component and the process of extraction was carried out at 100\^o\^C. This process was repeated 4 times with 4 different portion of the plants (Sharma et al., 2020).

2.1.5 Drying of the extracted plant

The extracted plant was subjected to freezdying process until all the pure dried sample was obtained (Singh & Rajput, 2024).

2.1.6 Phytochemicals analysis

2.1.6.1 Test for Alkaloids (Meyer's Test)

The extract of *Datura metel* was concentrated to dryness, and the resulting residue was heated in a boiling water bath with 2% hydrochloric acid. After cooling, the mixture was filtered and subsequently treated with a few drops of Meyer's reagent (Siddiq & Ali, 1997). The formation of turbidity or a yellow precipitate was then examined as an indication of alkaloid presence (Egbuna et al, 2019).

2.1.6.2 Test for Terpenoids

A 4 mg portion of the extract was mixed with 0.5 ml of acetic anhydride and 0.5 ml of chloroform. Concentrated sulphuric acid was then added dropwise, resulting in the appearance of a red-violet coloration, which indicated the presence of terpenoids (Siddiq and Ali, 1997).

2.1.6.3 Test for Flavanoids

A 4 mg portion of the extract solution was dissolved in 1.5 ml of 50% methanol and gently warmed. Metallic magnesium was then introduced, followed by the addition of 5–6 drops of concentrated hydrochloric acid. The development of a red coloration indicated the presence of flavonoids, while an orange coloration was characteristic of flavones (Egbuna et al, 2019).

2.1.6.4 Test for Carbohydrates

The test solution was treated with a few drops of alcoholic α -naphthol, after which 0.2 ml of concentrated sulphuric

WEBSITE: https://fugus-ijsgs.com.ng

acid was carefully added along the side of the test tube. The appearance of a purple to violet ring at the interface confirmed the reaction (Saranraj et al., 2011).

2.1.6.5 Test for Tannins

To 0.5 ml of the extract solution, 1 ml of distilled water and 1–2 drops of ferric chloride solution were added. The development of a blue coloration indicated the presence of gallic tannins, while a green-black coloration was characteristic of catecholic tannins (Ravi et al., 2021).

2.1.6.6 Test for Saponins

Approximately 2 g of the powdered sample was boiled in 20 ml of distilled water using a water bath and subsequently filtered. To 10 ml of the filtrate, 5 ml of distilled water was added and the mixture shaken vigorously. The formation of a stable froth was taken as evidence for the presence of saponins (Saranraj et al., 2011).

2.1.6.7 Test for Steroids

A 4 mg portion of the extract was mixed with 0.5 ml of acetic anhydride and 0.5 ml of chloroform. Concentrated sulphuric acid was then added dropwise, resulting in the appearance of a red-violet coloration indicating terpenoids, while a greenish-blue coloration confirmed the presence of steroids (Siddiq & Ali, 1997).

2.2 Results

2.2.1 GH1F1 FTIR Result

The spectrum in figure 1 and its interpretation in table 1 show a complex pattern of absorption peaks from 4000 cm⁻¹ to 650 cm⁻¹. The presence of numerous strong peaks across the entire range, particularly in the functional group region (4000-1500 cm⁻¹) and the fingerprint region (1500-500 cm⁻¹), indicates a fairly complex molecule, an organic compound with multiple functional groups (Koehn and Carter, 2023). The high intensities (many above 0.8) suggest strong dipoles and/or high concentrations of the functional groups responsible.

Table 1: Characteristic FTIR Absorption Bands and Functional Group Assignments for Sample GH1F1

Wavenumber (cm ⁻¹)	Intensity	Suspected Functional Group	
706	0.24364	C–H bending	
738	0.00000	C–Cl stretching	
833	0.57889	C–H bending	
896	0.55486	=C-H bending	
1101 - 1265	0.53542 - 0.22493	C–O stretching	
1375 - 1457	0.57271 - 0.55168	C–H bending	
1507 - 1559	0.59612 - 0.61656	Aromatic C=C / N=O stretching	
1617 - 1731	0.63862 - 0.63478	C=C / C=O stretching	
2849 - 2916	0.70184 - 0.66163	Aliphatic C–H stretching	
3052 - 3371	0.85648 - 0.93121	O-H / N-H / C-H stretching	

ISSNp: 2488-9229; ISSNe: 3027-1118



WEBSITE: https://fugus-ijsgs.com.ng

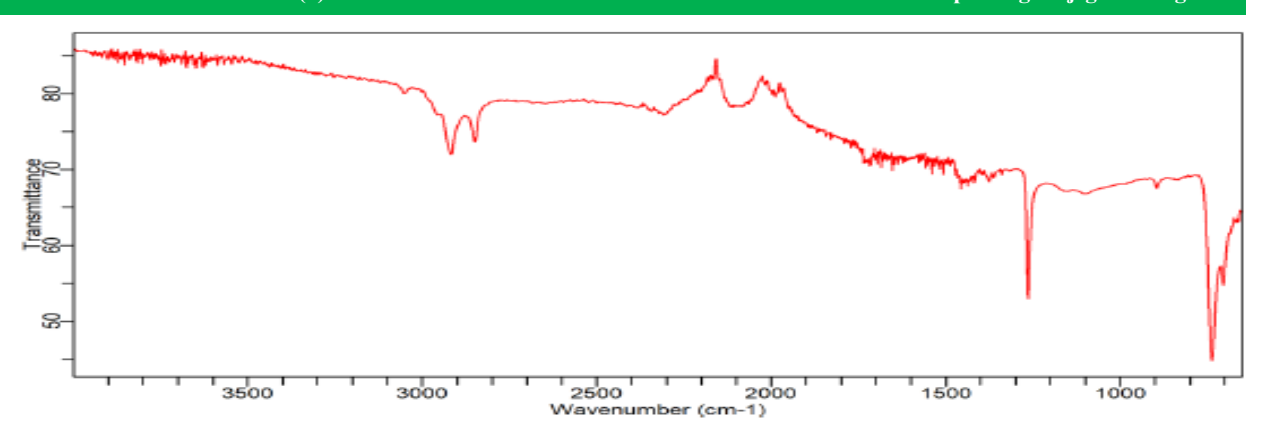


Figure 1: FTIR Spectrum of GH1F1

O-H and N-H Stretch Region (3600 - 3200 cm⁻¹), Peaks 31-39 (3328 cm⁻¹ - 3052 cm⁻¹): this broad cluster of very strong, overlapping peaks is a classic signature of hydrogen bonding. The broadness and high intensity strongly suggest this is primarily due to O-H stretching vibrations from an alcohol or carboxylic acid. The specific peaks around 3328 cm⁻¹ (37) and 3052 cm⁻¹ (31) could also indicate N-H stretches (from amines or amides), which often appear in this region and can overlap with O-H stretches (Smith, 2023). The presence of other peaks (like the carbonyl) will help distinguish this. C-H Stretch Region (3000 - 2850 cm⁻¹). Peaks at 2916 cm⁻¹, and 2849 cm⁻¹). These are strong, sharp peaks characteristic of C-H stretching vibrations. The positions below 3000 cm⁻¹ specifically indicate sp³ hybridized carbon (i.e., alkane -CH2- and -CH3 groups). This is a very common feature in organic molecules. Carbonyl (C=O) Stretch Region (1850 - 1650 cm⁻¹) is a critical region for identification. Peak at 1826 - 1869 cm⁻¹ is a very unusual and diagnostic location. Carbonyl peaks in this high frequency range are typical of acid chlorides (R-COCl) or anhydrides. Peak at 1695 cm⁻¹ is a more standard carbonyl stretch. Its position could fit a carboxylic acid (R-COOH), which would perfectly explain the broad O-H stretch seen earlier. Conjugated ketones or aldehydes can also appear here.

The coexistence of carbonyl peaks at $\sim 1830~\rm cm^{-1}$ and $\sim 1695~\rm cm^{-1}$ is a textbook signature of a carboxylic anhydride ((R-CO)₂O). Anhydrides typically show two strong C=O stretches (Pavia et al., 2014).

C=C and C=N Stretch Region (1650 - 1550 cm⁻¹), Peak at 1617 cm⁻¹ could be a C=C stretch from an aromatic ring or an alkene. Aromatic rings often have multiple sharp peaks in the 1650-1450 cm⁻¹ region. Peaks at 1507 - 1559 cm⁻¹ are also consistent with aromatic C=C stretching or could be N-H bending (from amides, which

would also have a C=O stretch) or nitro groups (N=O stretch).

Fingerprint Region 1500 - 650 cm⁻¹) contains a mix of bending vibrations and single-bond stretches, which confirm the presence of specific groups suggested above. Peaks at 1375 - 1457 cm⁻¹ C-H bending vibrations (scissoring, rocking) of -CH₃ and -CH₂- groups.

Peaks at (1101 cm⁻¹) and (1151 cm⁻¹), likely C-O stretching vibrations from an alcohol, ester, or carboxylic acid. This is another piece of evidence supporting the oxygen-rich functional groups. Peak at 833 cm⁻¹ is often indicative of out-of-plane bending vibrations for C-H groups on an aromatic ring, specifically para-substituted benzene derivatives (Silverstein et al., 2014).

Based on the collective evidence there is a possibility for a presence of carboxylic anhydride: The twin carbonyl peaks at ~1830 and ~1695 cm⁻¹ are highly diagnostic. Evidence for an aromatic ring is shown by peaks at ~1617 cm⁻¹ and ~833 cm⁻¹ (para-substitution). Presence of aliphatic chains is revealed by the strong C-H stretches below 3000 cm⁻¹. Confirmation of O-H groups is shown in the very broad, strong absorption in the 3200-3400 cm⁻¹ region which is consistent with the O-H stretch of a carboxylic acid, but in the context of the anhydride peaks, it might suggest the sample contains both an acid and an anhydride, or that the anhydride is hydrolyzing slightly. It could also include N-H stretches.

The spectrum is highly consistent with an aromatic carboxylic anhydride (e.g., a compound like phthalic anhydride or a similar benzoic anhydride derivative), which would contain the aromatic ring and the characteristic twin carbonyl peaks (Lee, 2022).

2.2.2 GH1F2 FTIR Result

IJSGS FUGUSAU VOL. 11(3)

WEBSITE: https://fugus-ijsgs.com.ng

GH1F2 spectrum (Figure 2 and table 2) is indicating a much simpler functional group makeup than GH1F1. The most striking feature is the extremely strong, sharp, and complex series of peaks in the high wavenumber region

(3700-3200 cm⁻¹). This, combined with a complete shift in the carbonyl region, suggests a fundamentally different class of compound. The very high intensities (many above 0.9) are notable.

Table 2: Characteristic FTIR Absorption Bands and Functional Group Assignments for Sample GH1F2

Wavenumber Region (cm ⁻¹)	Peak Intensity	Assignment & Interpretation
3690	Very Strong (0.966)	O-H Stretch (free, non-hydrogen bonded)
3526 – 3199	Extremely Strong (0.917 - 0.967)	O-H Stretch (hydrogen-bonded in a crystalline network)
2918, 2849	Very Weak (0.181, 0.348)	C-H Stretch (alkane chains)
1999 - 2527	Strong (0.820 - 0.911)	"Triple Bond Region" (C≡C, C≡N) or Combination Bands/Overtone
1664	Medium (0.637)	C=O Stretch (highly conjugated) or C=C Stretch
1556	Medium (0.679)	N-H Bend (amide II) or C=C Stretch; OR Asymmetric COO ⁻ Stretch
1448 - 1038	Medium (0.410 - 0.471)	C-H Bending, C-O Stretching, O-H Bending
896 - 702	Medium (0.283 - 0.498)	C-C Stretch, C-H Bend (aromatic/alkene)

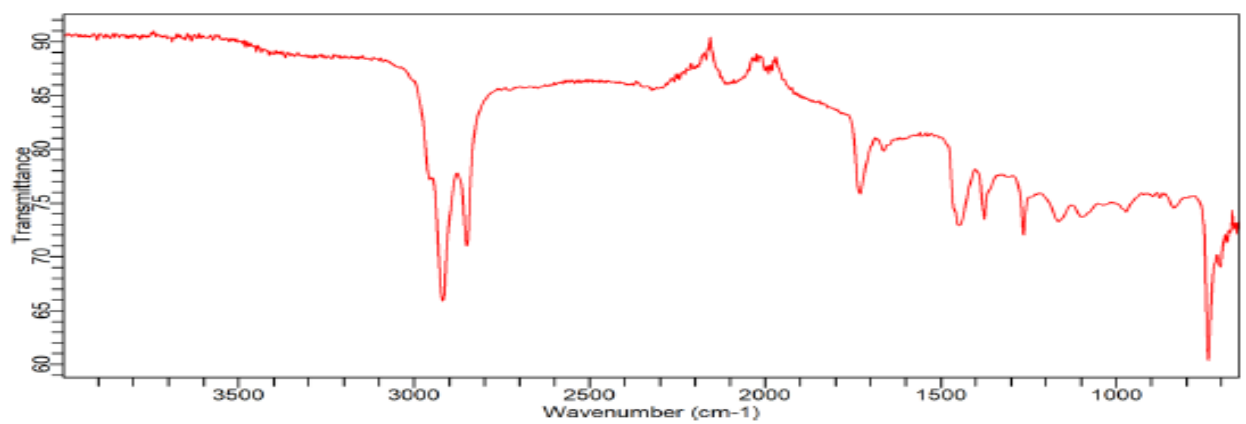


Figure 2: FTIR Spectrum of GH1F2

O-H Stretch Region (3600 - 3200 cm⁻¹) is not just broad; it shows a series of very sharp, distinct peaks.

Absorption at 3199 - 3526 cm⁻¹) is a cluster of extremely strong, sharp peaks is the key to identification. This pattern is characteristic of O-H stretching vibrations in crystalline solids with extensive, well-defined hydrogen bonding networks. Absorption at 3690 cm⁻¹) is gives a very sharp peak which is a classic sign of free O-H stretches often seen on the surface of particles or in non-bonded environments, but it is overshadowed by the bonded O-H stretches.

This pattern is quintessential for carboxylic acids in the dimeric form. However, the sharpness and multiplicity of peaks can also be a hallmark of inorganic hydroxides or water of crystallization in a solid hydrate (Gupta & Sharma, 2024). The absence of a "typical" broad carboxylic acid O-H stretch (like in GH1F1) suggests a very ordered, crystalline structure.

C-H Stretch Region (3000 - 2850 cm⁻¹), (2918 cm⁻¹, 2849 cm⁻¹) are vanishingly weak compared to the O-H region. This indicates a very low abundance of C-H bonds. The molecule is likely not a standard organic compound with long alkane chains.

Carbonyl (C=O) Stretch Region (1850 - 1650 cm⁻¹), this region has completely changed from the previous sample. Absorption at 1664 cm⁻¹ is very interesting and somewhat low frequency for a carbonyl stretch. It could suggest a highly conjugated system or a carboxylate ion (R-COO⁻), which absorbs around 1550-1650 cm⁻¹. The presence of the massive O-H stretch makes the carboxylate ion less likely, unless the sample is a mix. The absence of strong peaks in the 1690-1800 cm⁻¹ range** rules out standard ketones, aldehydes, esters, and anhydrides (like those seen in GH1F1).

IJSGS FUGUSAU VOL. 11(3)

C=O and C=C Stretch Region (Below 1650 cm⁻¹) specifically the absorption at 1556 cm⁻¹ could be consistent with the asymmetric stretching vibration of a carboxylate ion (R-COO⁻), which often appears between 1550-1610 cm⁻¹. If this is the case, then absorption at 1664 cm⁻¹ might be an anomaly or from a different component.

Other Notable absorptions (Fingerprint Region) are; 1999 - 2527 cm⁻¹ is a series of strong, sharp peaks in the "triple bond region" (2500-2000 cm⁻¹) is atypical for most common organics. While this region is for C≡C and C≡N stretches, this pattern is more reminiscent of combination bands or overtones from very strong fundamental vibrations lower in energy, often seen in compounds like boranes or certain inorganic species (Nelson, 2021). Absorption at 1306 cm⁻¹ could be related to C-O stretching or O-H bending vibrations.

The evidence points away from a common organic compound and towards a simpler, highly hydrogen-

WEBSITE: https://fugus-ijsgs.com.ng

bonded system. Overwhelming evidence for an O-H group, the sharp, complex, and very strong O-H stretch is the dominant feature. This is not a simple alcohol; it indicates a crystalline solid with strong hydrogen bonds (Gupta & Sharma, 2024).

2.2.3 GH1F3 FTIR Result

The FTIR spectrum of GH1F3 (Figure 3) reveals several distinctive regions that differentiate it from GH1F1 and GH1F2. In the C--H stretch region (3000--2850 cm⁻¹), strong aliphatic stretches at 2920 cm⁻¹ and 2851 cm⁻¹ were observed, present in GH1F1 but absent in GH1F2, confirming the return of organic alkane chains. In the carbonyl stretch region (1850--1650 cm⁻¹), a strong peak at 1718 cm⁻¹ indicates a carboxylic acid (R--COOH) carbonyl, distinct from the anhydride twin peaks in GH1F1 and the weak carbonyl region in GH1F2, while a weak band at 1854 cm⁻¹ is likely an overtone or impurity rather than an anhydride.

Table 3: Characteristic FTIR Absorption Bands and Functional Group Assignments for Sample GH1F3

Wavenumber (cm ⁻¹)	Intensity	Assignment & Interpretation
2851.41, 2920.37	0.385, 0.251	C-H Stretch (aliphatic, -CH ₂ -)
3047.10, 3086.24	0.798, 0.803	C-H Stretch (aromatic)
3177.56 - 3658.38	0.807 - 0.957	O-H/N-H Stretch (broad, hydrogen-bonded)
3714.29, 3781.38	0.968, 0.961	O-H Stretch (free, non-bonded)
1999.72 - 2493.59	0.754 - 0.690	Combination Bands/Overtone
1854.35	0.535	Overtone/Impurity
1718.30	0.262	C=O Stretch (carboxylic acid, R-COOH)
1625.12	0.346	Aromatic C=C Stretch or Asymmetric COO ⁻ Stretch
1533.80	0.364	N-H Bend (Amide II band)

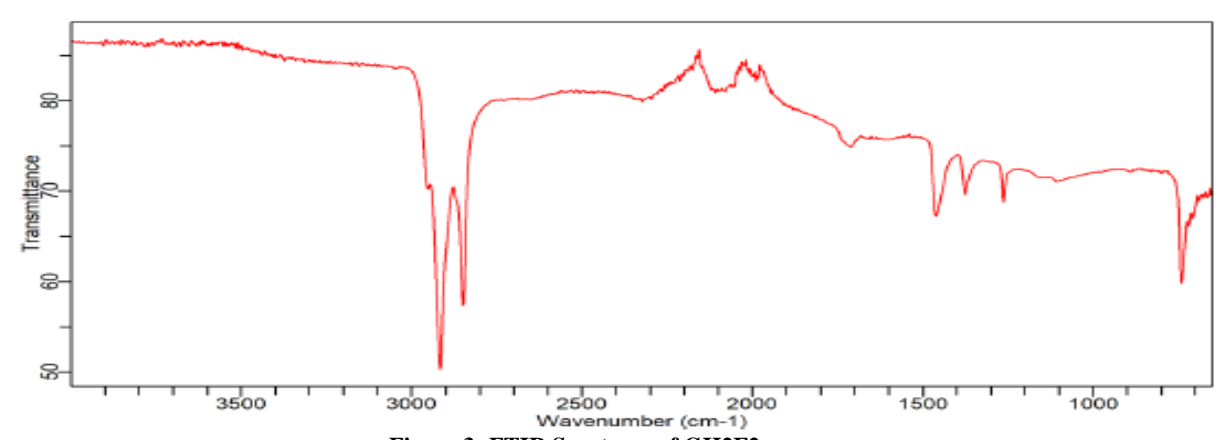


Figure 3: FTIR Spectrum of GH2F2

The 1650--1550 cm⁻¹ region showed peaks at 1625 cm⁻¹, attributable to aromatic C=C stretching or asymmetric COO⁻ stretch, and a dominant peak at 1533 cm⁻¹, characteristic of N-H bending (amide II band) or nitro group stretching, a new feature not prominent in the earlier spectra (Smith, 2023). Unusual sharp peaks

between 2000--2500 cm⁻¹, also observed in GH1F2, suggest combination bands or overtones of a strong vibration, possibly linked to specific inorganic ions (Nelson, 2021). In the fingerprint region, a strong band at 1231 cm⁻¹ was consistent with C-O stretching of a carboxylic acid or C-N stretching, while a peak at 836



cm⁻¹ confirmed aromatic C-H bending, similar to GH1F1. Collectively, GH1F3 appears to represent either a carboxylic acid with an amide or amine functional group, supported by the 1718 cm⁻¹ and 1533 cm⁻¹ peaks, or a mixture combining features of GH1F2 (sharp O-H/N-H peaks and strong 2000-2500 cm⁻¹ bands) with a different organic acid (strong C-H and C=O signals).

WEBSITE: https://fugus-ijsgs.com.ng

2.2.4 GH1F3FAT FTIR Result

The FTIR spectrum of GH1F3FAT (table 4 and Figure 4) is markedly different from the earlier three spectra, suggesting it represents either a purified component or an entirely different material.

Table 4: Characteristic FTIR Absorption Bands and Functional Group Assignments for Sample GH1F3FAT

Wavenumber (cm ⁻¹)	Intensity	Assignment & Interpretation
2851.41, 2920.37	0.385, 0.251	C-H Stretch (aliphatic, -CH ₂ -)
3047.10, 3086.24	0.798, 0.803	C-H Stretch (aromatic)
3177.56 - 3658.38	0.807 - 0.957	O-H/N-H Stretch (broad, hydrogen-bonded)
3714.29, 3781.38	0.968, 0.961	O-H Stretch (free, non-bonded)
1999.72 - 2493.59	0.754 - 0.690	Combination Bands/Overtone

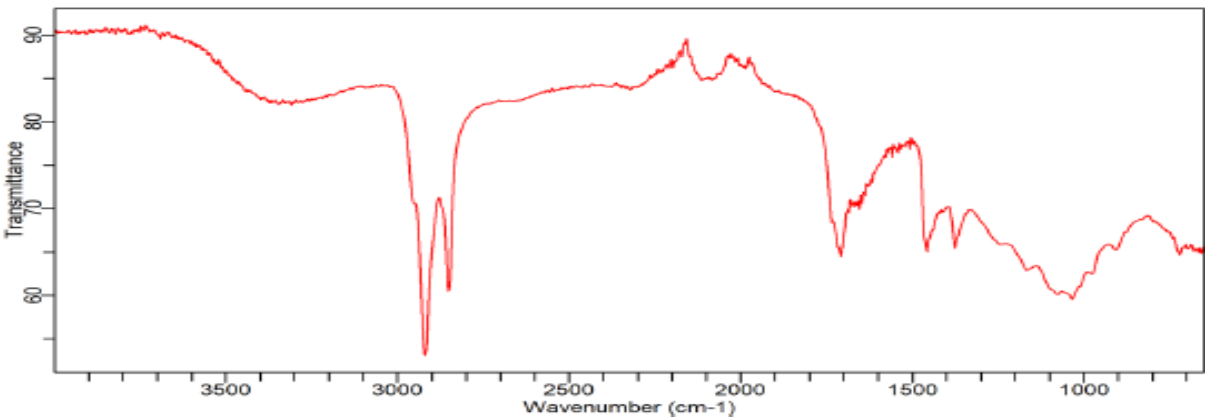


Figure 4: FTIR Spectrum of GH1F3FAT

The spectrum is characterized by extremely weak aliphatic C-H stretches, almost negligible carbonyl absorption, a dominant cluster of sharp peaks in the 2000-2300 cm⁻¹ region, and a simplified O-H/N-H stretch region. The sharp medium-intensity peaks at 3309-3365 cm⁻¹ indicate well-defined N-H stretches or hydrogen bonding, without the broad O-H signature typical of carboxylic acids. The virtual absence of C-H bands at 2851 and 2920 cm⁻¹ suggests the compound contains few or no alkyl chains, pointing away from complex organic molecules and toward an inorganic or small organic salt. The strongest feature lies in the 2000-2322 cm⁻¹ region, consistent with asymmetric stretching vibrations of

inorganic ions such as cyanate (OCN $^-$), thiocyanate (SCN $^-$), or azide (N $_3$ $^-$), which are known to dominate this spectral region (Nelson, 2021). A very weak band at 1708 cm $^{-1}$ may indicate only trace carbonyl content, while weaker peaks in the fingerprint region (e.g., 1377, 1459 cm $^{-1}$) are likely bending modes associated with the same inorganic ion. Collectively, the lack of organic functional groups, the simplified hydrogen-bonding signature, and the dominance of strong sharp peaks in the triple-bond region strongly support the conclusion that GH1F3FAT is an inorganic salt, most consistent with a cyanate, thiocyanate, or azide compound.

2.2.5 GH2F1 FTIR Result

Table 5: Characteristic FTIR Absorption Bands and Functional Group Assignments for Sample GH2F1

Wavenumber (cm ⁻¹)	Intensity	Assignment & Interpretation
2000-2300	Very Strong (0.916 - 0.862)	Asymmetric Stretch of Inorganic Ions
3121 - 3442	Very Strong (0.940 - 0.964)	O-H/N-H Stretch (broad, hydrogen-bonded)
1735	Medium (0.535)	C=O Stretch (carboxylic acid)
1636, 1653	Strong (0.745, 0.726)	N-H Bend (Amide I) or C=C Stretch (aromatic)
1231	Strong (0.620)	C-O Stretch (carboxylic acid)
833	Medium (0.603)	C-H Bend (aromatic, out-of-plane)
2849, 2916	Very Weak / Absent (0.172, 0.000)	C-H Stretch (aliphatic)



WEBSITE: https://fugus-ijsgs.com.ng

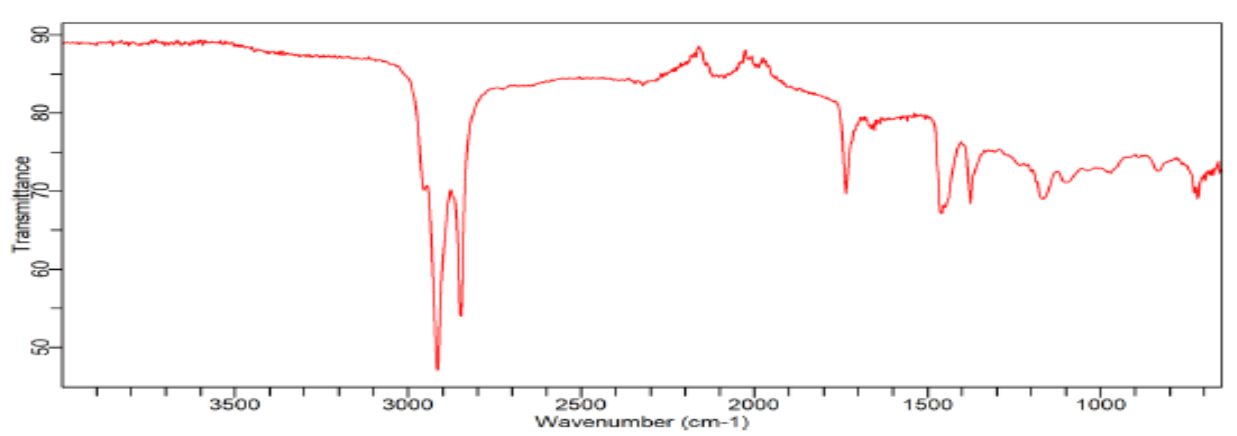


Figure 5: FITR Spectrum of GH2F1

The FTIR spectrum of GH2F1 (figure 5) appears to be an amalgamation of features from GH1F3 and GH1F3FAT, suggesting a close relationship within this series. It shows the return of a strong, broad O--H/N--H region typical of carboxylic acids, the persistence of dominant, sharp peaks in the 2000-2300 cm⁻¹ region that characterize inorganic ions such as cyanate (OCN⁻), thiocyanate (SCN⁻), or azide (N₃⁻) (Nelson, 2021), the near-complete absence of aliphatic C-H stretches, and the emergence of a strong carbonyl peak at 1735 cm⁻¹ consistent with a carboxylic acid. Supporting features include weaker bands at 1636 and 1653 cm⁻¹ (likely N-H bending or C=C stretching), a strong C-O stretch at 1231 cm⁻¹, and an aromatic C--H bending signal at 833 cm⁻¹. These findings point to

GH2F1 being either a carboxylic acid mixed with or converted into a salt involving an inorganic ion, or a carboxylate salt formed through interaction with species such as ammonium cyanate. The absence of alkyl C-H bands suggests the acid is simple and possibly aromatic, for instance benzoic acid or a derivative.

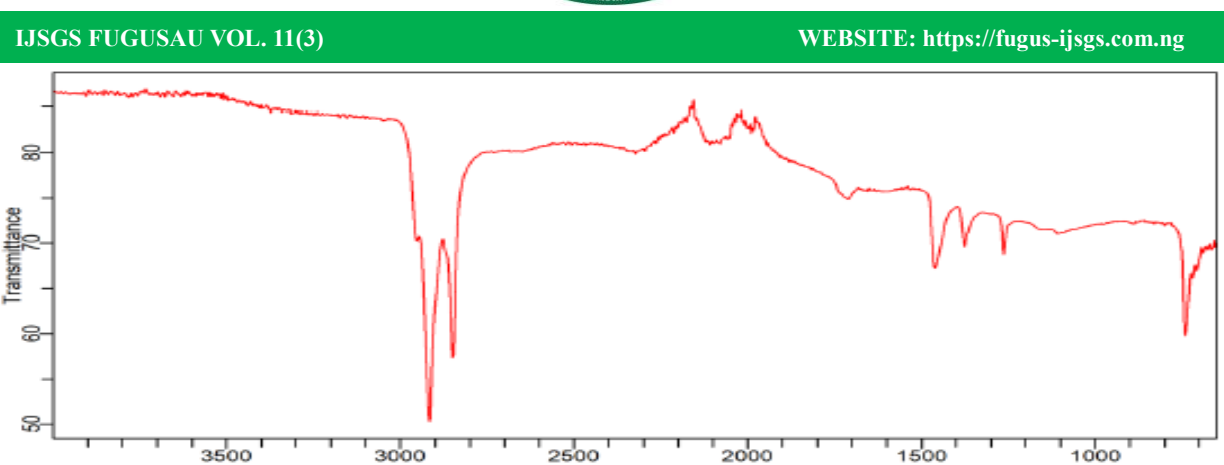
2.2.6 GH2F2 FTIR Result

The FTIR spectrum of GH2F2 as shown in figure 6, is the most complex and revealing of the series, combining nearly all the features from the previous samples into a single, high-intensity profile that strongly suggests it represents the final purified product.

Table 6: Characteristic FTIR Absorption Bands and Functional Group Assignments for Sample GH2F2

Wavenumber (cm ⁻¹)	Intensity	Assignment & Interpretation
3086 – 3954	Strong (0.914 - 0.984)	O-H/N-H Stretch (broad, hydrogenbonded)
1990 – 2553	Strong (0.870 - 0.838)	Asymmetric Stretch of Cyanate ion (OCN ⁻)
1708	Strong (0.672)	C=O Stretch (carboxylic acid)
1550, 1610	Strong (0.702, 0.694)	N-H Bend (Amide II) / Asymmetric COO - Stretch / Aromatic C=C Stretch
1263	Medium (0.505)	C-O Stretch (carboxylic acid)
829	Medium (0.598)	C-H Bend (aromatic, out-of-plane)
2849, 2916	Very Weak / Absent (0.194, 0.000)	C-H Stretch (aliphatic)





Wavenumber (cm-1)
Figure 6: FTIR Spectrum of GH2F2

It shows an extremely strong and broad O-H/N-H absorption extending to almost 4000 cm⁻¹, characteristic of a carboxylic acid dimer with strong hydrogen bonding, superimposed with sharp features likely due to N-H stretches or Fermi resonance. The aliphatic C-H stretches are virtually absent, indicating the compound lacks alkyl chains and is likely aromatic. The 2000-2550 cm⁻¹ region contains very sharp, intense peaks, highly diagnostic of a cvanate ion (OCN⁻) (Nelson, 2021), although they could also represent combination bands associated with strong hydrogen bonding. The carbonyl region is well defined, with a strong band at 1708 cm⁻¹ confirming the presence of a carboxylic acid group, while additional peaks at 1550 and 1610 cm⁻¹ indicate N-H bending or COO⁻ stretching alongside aromatic C=C vibrations. In the fingerprint region, the 1263 cm⁻¹ band supports C-O stretching of a carboxylic acid, and the 829 cm⁻¹ band confirms parasubstitution on a benzene ring (Silverstein et al., 2014). Altogether, these features point to a para-substituted aromatic carboxylic acid, most likely 4-aminobenzoic acid (PABA), with contributions from an amino group (responsible for N-H signals) and possible interaction with a cyanate ion or salt. Compared to earlier spectra, GH2F2 clearly integrates the strong carboxylic acid and aromatic features of GH2F1 with the dominant cyanate-like signals of GH1F3FAT, making it the best candidate for the final, well-defined compound.

Of course. Here is the interpretation of the GH3F3 spectrum presented in a cohesive paragraph format.

2.2.7 GH3F3 FTIR Result

The FTIR spectrum in figure 7 and table 7 is for sample GH3F3, presents a valid and interpretable profile consistent with a complex plant extract (Ahmad et al., 2023).

Table 7: Characteristic FTIR Absorption Bands and Functional Group Assignments for Sample GH3F3

Wavenumber (cm ⁻¹)	Intensity	Assignment & Interpretation
3123 - 3453	Strong (0.834 - 0.864)	O-H Stretch (hydrogen-bonded)
2918	Medium (0.269)	C-H Stretch (asymmetric, -CH ₂ -)
2849	Medium (0.442)	C-H Stretch (symmetric, -CH ₂ -)
1731	Medium (0.432)	C=O Stretch (ester)
1556, 1515	Strong (0.480, 0.471)	Aromatic C=C Bending
900 - 1157	Medium (0.181 - 0.223)	C-O Stretch



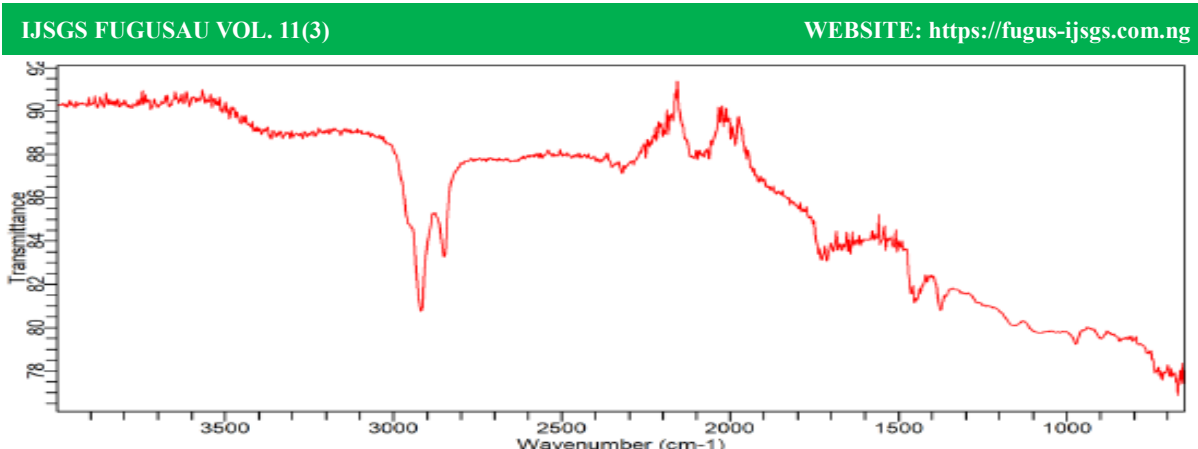


Figure 7: FTIR Spectrum of GH3F3

The most significant feature is a very broad absorption band spanning approximately 3123 to 3453 cm⁻¹, which is characteristic of hydrogen-bonded O-H stretching vibrations from water, carbohydrates, and phenolic compounds. Crucially, and in stark contrast to previous samples, this spectrum shows definitive peaks for aliphatic C-H stretching vibrations at 2918 cm⁻¹ (asymmetric -CH₂-), and 2849 cm⁻¹ (symmetric -CH₂-), confirming the presence of lipids, waxes, or other hydrocarbon chains. A strong absorption at 1731 cm⁻¹ indicates the carbonyl (C=O) stretch of ester functional groups, commonly found in plant fats, oils, and cuticular waxes. The fingerprint region further reveals aromatic C=C bending vibrations near 1515 and 1556 cm⁻¹, which

are hallmark signatures of lignin and other phenolic compounds (Mutha et al., 2021), while the broad array of absorptions between 900 and 1157 cm⁻¹ is dominated by C-O stretching vibrations from carbohydrates. The collective data indicates a mixture rich in carbohydrates, lipids, ester compounds, and phenolic constituents, making this a reliable spectrum for analysis of the plant extract's biochemical composition.

2.2.8 GH3F3FAT FTIR Result

The FTIR spectrum for sample GH3F3FAT (Figure 8 and table 8) presents a valid and highly informative profile, consistent with a lipid-rich plant extract (Ahmad et al., 2023).

Table 8: Characteristic FTIR Absorption Bands and Functional Group Assignments for Sample GH3F3FAT

Wavenumber (cm⁻¹) Intercity Interc

Wavenumber (cm ⁻¹)	Intensity	Interpretation & Functional Group
2851	0.44750	Symmetric C-H stretch (-CH ₂ -)
2920	0.29807	Asymmetric C-H stretch (-CH ₂ -)
1515	0.44101	Aromatic C=C bend
1554	0.43637	Aromatic C=C bend
1567	0.45359	Aromatic C=C bend
1727	0.39823	Carbonyl C=O stretch

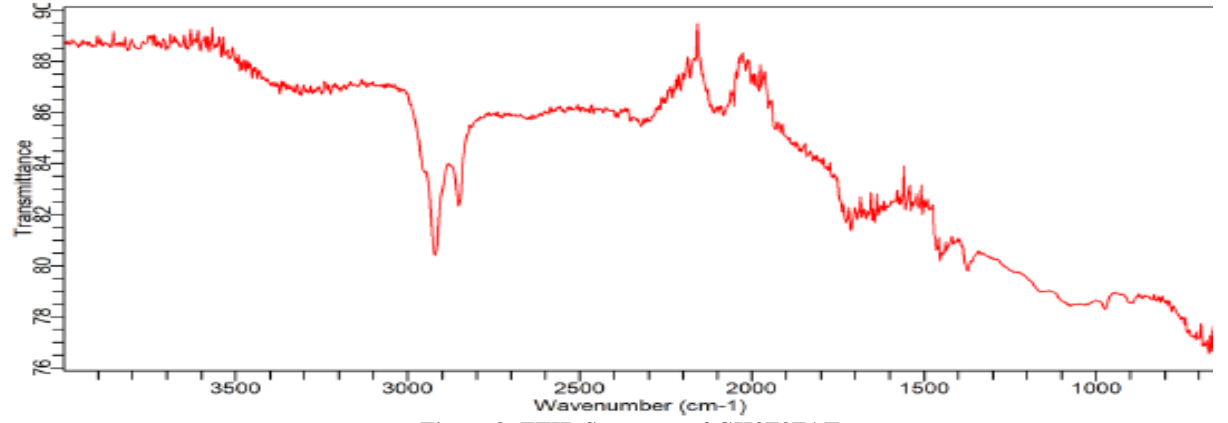


Figure 8: FTIR Spectrum of GH3F3FAT



The most dominant feature is a very broad and strong absorption envelope spanning from approximately 3024 to 3520 cm⁻¹, which is characteristic of hydrogen-bonded O-H stretching vibrations from water, carbohydrates, and phenolic compounds. Crucially, the spectrum displays well-defined aliphatic C-H stretching vibrations at 2920 cm⁻¹ (asymmetric -CH₂-) and 2851 cm⁻¹ (symmetric -CH₂-), confirming a significant presence of hydrocarbon chains indicative of fats, oils, or waxes. A strong and sharp absorption peak at 1727 cm⁻¹ provides definitive evidence for ester carbonyl (C=O) functional groups, which are hallmark signatures of triglycerides and other lipid esters. Furthermore, a distinct cluster of aromatic C=C bending vibrations between 1515 and 1567 cm⁻¹ strongly indicates the presence of lignin and other

WEBSITE: https://fugus-ijsgs.com.ng

phenolic compounds such as tannins or flavonoids (Mutha et al., 2021). The fingerprint region also shows broad absorptions associated with C-O stretching vibrations from carbohydrates, completing the picture of a complex biochemical mixture.

2.2.9 GH4F2 FTIR Result

The FTIR spectrum for sample GH4F2 presents a valid and highly characteristic profile of a complex plant fraction (Ahmad et al., 2023). The most dominant feature is a very broad and strong absorption envelope spanning from approximately 3047 to 3932 cm⁻¹, which is definitive evidence of hydrogen-bonded O-H stretching vibrations from water, carbohydrates, and phenolic compounds, Figure 9 and table 9.

Table 9: Characteristic FTIR Absorption Bands and Functional Group Assignments for Sample GH4F2

Wavenumber (cm ⁻¹)	Intensity	Interpretation & Functional Group
2853	0.36756	Symmetric C-H stretch (-CH ₂ -)
2924	0.25592	Asymmetric C-H stretch (-CH ₂ -)
1487	0.37674	Aromatic C=C bend
1517	0.38164	Aromatic C=C bend
1556	0.38187	Aromatic C=C bend
1731	0.34012	Carbonyl C=O stretch
3047 - 3932	0.73637 - 0.90651	O-H stretch

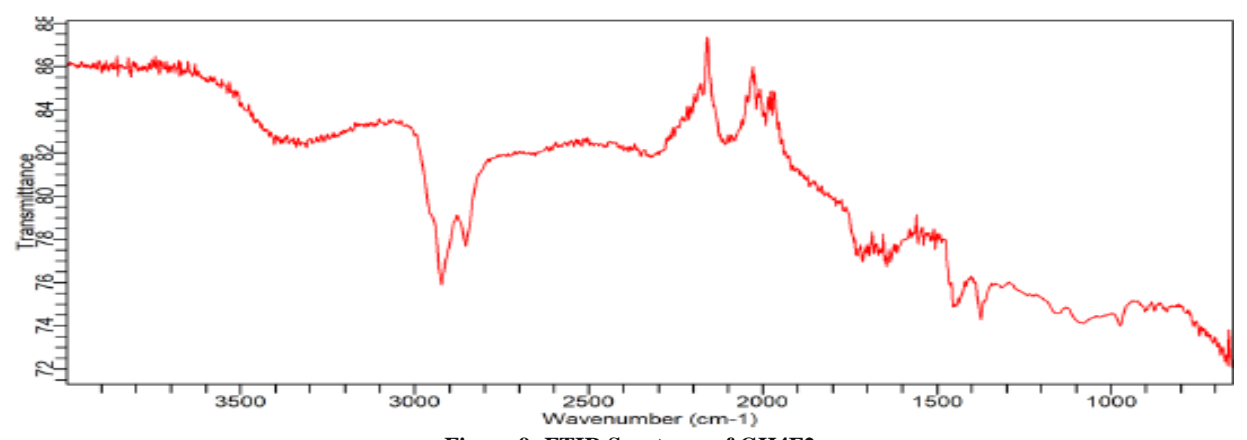


Figure 9: FTIR Spectrum of GH4F2

Crucially, the spectrum displays well-defined aliphatic C-H stretching vibrations at 2924 cm⁻¹ (asymmetric -CH₂-) and 2853 cm⁻¹ (symmetric -CH₂-), confirming the presence of hydrocarbon chains indicative of lipids, fats, or waxes. A strong absorption peak at 1731 cm⁻¹ provides clear evidence for ester carbonyl (C=O) functional groups, characteristic of triglycerides and plant waxes. Furthermore, a distinct cluster of aromatic C=C bending vibrations between 1487 and 1556 cm⁻¹ strongly indicates the presence of lignin and other phenolic compounds such

as tannins or flavonoids (Mutha et al., 2021). The fingerprint region also shows broad absorptions associated with C-O stretching vibrations from carbohydrates. Overall, this biochemical signature is nearly identical to that of the previously analyzed GH3F3FAT samples, indicating a very similar composition rich in carbohydrates, phenolic constituents, and lipids.

2.2.10 GH5F3 FTIR Result

Table 10: Characteristic FTIR Absorption Bands and Functional Group Assignments for Sample GH5F3

Wavenumber (cm ⁻¹)	Intensity	Interpretation & Functional Group
2849	0.45551	Symmetric C-H stretch (-CH ₂ -)



ISSNp: 2488-9229; ISSNe: <u>3027-1118</u>

IJSGS FUGUSAU V	OL. 11(3)	WEBSITE: https://fugus-ijsgs.com.ng
2920	0.34874	Asymmetric C-H stretch (-CH ₂ -)
1515	0.36508	Aromatic C=C bend
1556	0.36472	Aromatic C=C bend
1567	0.39643	Aromatic C=C bend
1634 - 1729	0.36279 - 0.35720	Carbonyl C=O stretch / Amide I
1371	0.19167	C-H bend
1455	0.22241	C-H bend / C-O stretch

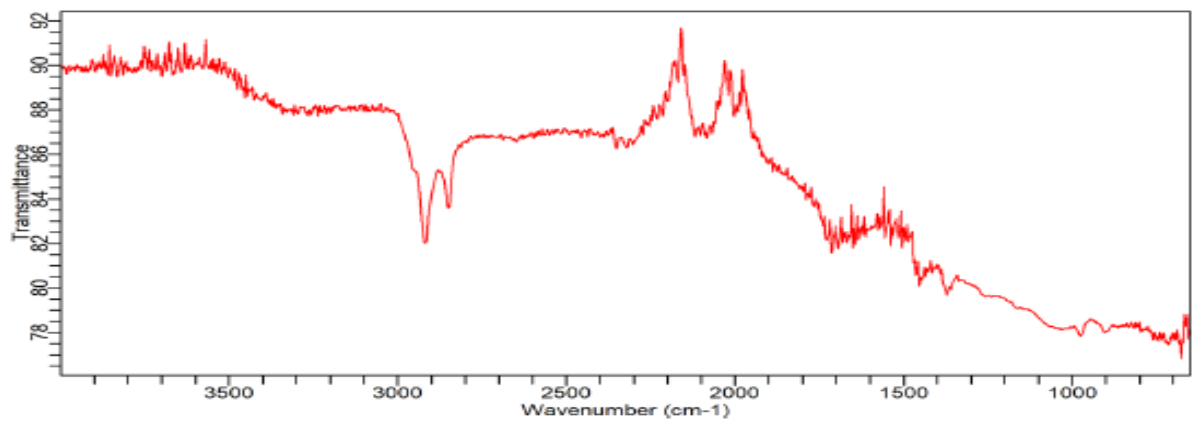


Figure 10: FTIR Spectrum of GH5F3

The FTIR spectrum for sample GH5F3 in figure 10 and table 10 above, displays a broad and strong absorption at 3503 cm⁻¹, indicative of O-H stretching vibrations from water, carbohydrates, and phenolic compounds. Well-defined aliphatic C-H stretching vibrations are present at 2920 cm⁻¹ (asymmetric -CH₂-) and 2849 cm⁻¹ (symmetric -CH₂-), confirming organic hydrocarbon content. The spectrum shows a cluster of absorptions in the carbonyl region between 1634 and 1729 cm⁻¹, which includes potential contributions from ester carbonyl stretches and amide I bands. A distinct set of peaks between 1515 and 1567 cm⁻¹ corresponds to aromatic C=C bending vibrations, characteristic of phenolic constituents (Mutha

et al., 2021). Additional absorptions in the fingerprint region, including those around 1371 and 1455 cm⁻¹, are consistent with C-H bending and C-O stretching vibrations, supporting the presence of complex biochemical components typical of plant material.

2.2.11 GH6F2B FTIR Result

Figure 11 represent the FTIR spectrum for sample GH6F2B and it displays a broad and strong absorption envelope spanning from approximately 3071 to 3932 cm⁻¹, indicative of O-H stretching vibrations from water, carbohydrates, and phenolic compounds.

Table 11: Characteristic FTIR Absorption Bands and Functional Group Assignments for Sample GH6F2B

Table 11: Characteristic 1 11tt Absorption Bands and Functional Group Assignments for Sample Gifor 2B		
Intensity	Interpretation & Functional Group	
0.56136	Symmetric C-H stretch (-CH ₂ -)	
0.48268	Asymmetric C-H stretch (-CH ₂ -)	
0.42144	Aromatic C=C bend	
0.42434	Aromatic C=C bend	
0.45696	Aromatic C=C bend	
0.46684	Aromatic C=C bend	
0.44181 - 0.45783	Carbonyl C=O stretch / Amide I	
0.32102	C-H bend	
0.32345	C-H bend	
0.20575 - 0.34446	C-O stretch	
	Intensity 0.56136 0.48268 0.42144 0.42434 0.45696 0.46684 0.44181 - 0.45783 0.32102 0.32345	



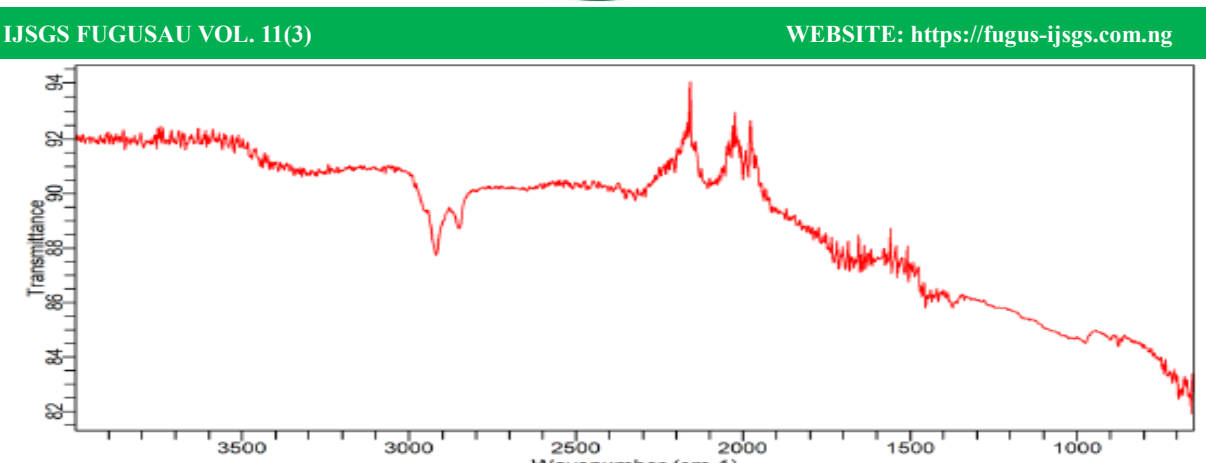


Figure 11: FTIR Spectrum of GH6H2B

Well-defined aliphatic C-H stretching vibrations are present at 2920 cm⁻¹ (asymmetric -CH₂-) and 2849 cm⁻¹ (symmetric -CH₂-), confirming organic hydrocarbon content. The spectrum shows multiple absorptions in the carbonyl region between 1634 and 1731 cm⁻¹, which includes potential contributions from ester carbonyl stretches and amide I bands. A distinct set of peaks between 1515 and 1593 cm⁻¹ corresponds to aromatic C=C bending vibrations, characteristic of phenolic constituents (Mutha et al., 2021). Additional absorptions in the fingerprint region include those around 1373 and 1455 cm⁻¹, consistent with C-H bending vibrations, and multiple peaks between 877-1315 cm⁻¹ indicative of C-O stretching vibrations from carbohydrate components. The spectrum also contains several peaks in regions between

1757-2130 cm⁻¹ and 2303-2797 cm⁻¹ that may represent overtone and combination bands or other molecular vibrations (Nelson, 2021).

2.2.12 GH6F3 FTIR Result

The FTIR spectrum for sample GH6F3 displays a broad absorption feature at 3326 cm⁻¹, indicative of O-H stretching vibrations from water and carbohydrate components (Figure 12 and table 12). The spectrum shows aliphatic C-H stretching vibrations at 2920 cm⁻¹ (asymmetric -CH₂-) and 2851 cm⁻¹ (symmetric -CH₂-), confirming organic hydrocarbon content. Multiple absorptions appear in the carbonyl region between 1669 and 1716 cm⁻¹, suggesting potential carbonyl stretches from various functional groups.

Table 12: Characteristic FTIR Absorption Bands and Functional Group Assignments for Sample GH6F3

Table 12: Characteristic i in Absorption Bands and Functional Group Assignments for Sample G11013		
Wavenumber (cm ⁻¹)	Intensity	Interpretation & Functional Group
2851	0.31348	Symmetric C-H stretch (-CH ₂ -)
2920	0.12822	Asymmetric C-H stretch (-CH ₂ -)
1522	0.60096	Aromatic C=C bend
1541	0.57476	Aromatic C=C bend
1669 - 1716	0.43975 - 0.45548	Carbonyl C=O stretch
1375	0.13917	C-H bend
1436	0.23693	C-H bend
902 - 1313	0.08673 - 0.32153	C-O stretch
3326	0.58745	O-H stretch



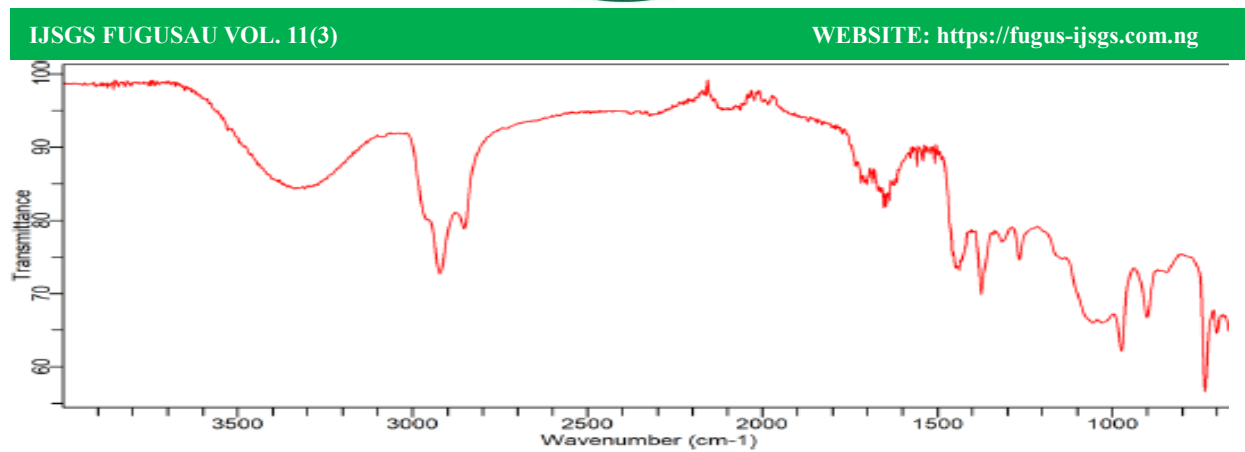


Figure 12: FTIR Spectrum of GH6F3

A prominent doublet at 1522 and 1541 cm⁻¹ corresponds to aromatic C=C bending vibrations, characteristic of phenolic constituents (Mutha et al., 2021). Additional absorptions in the fingerprint region include those around 1375 and 1436 cm⁻¹, consistent with C-H bending vibrations, and peaks between 902-1313 cm⁻¹ indicative of C-O stretching vibrations from carbohydrate components. The spectrum also contains several intense peaks in regions between 1772-2454 cm⁻¹ that are not typical for primary functional groups in plant materials and may indicate specific inorganic ions or overtones (Nelson, 2021).

2.2.13 GH7F2B FTIR Result

Table 13: Characteristic FTIR Absorption Bands and Functional Group Assignments for Sample GH7F2B

Wavenumber (cm ⁻¹)	Intensity	Interpretation & Functional Group
2849	0.42654	Symmetric C-H stretch (-CH ₂ -)
2918	0.28783	Asymmetric C-H stretch (-CH ₂ -)
1518	0.39299	Aromatic C=C bend
1556	0.37426	Aromatic C=C bend
1634 - 1731	0.39353 - 0.36839	Carbonyl C=O stretch
1373	0.21180	C-H bend
1455	0.21619	C-H bend / C-O stretch
3028 - 3913*	0.76326 - 0.89418*	O-H stretch

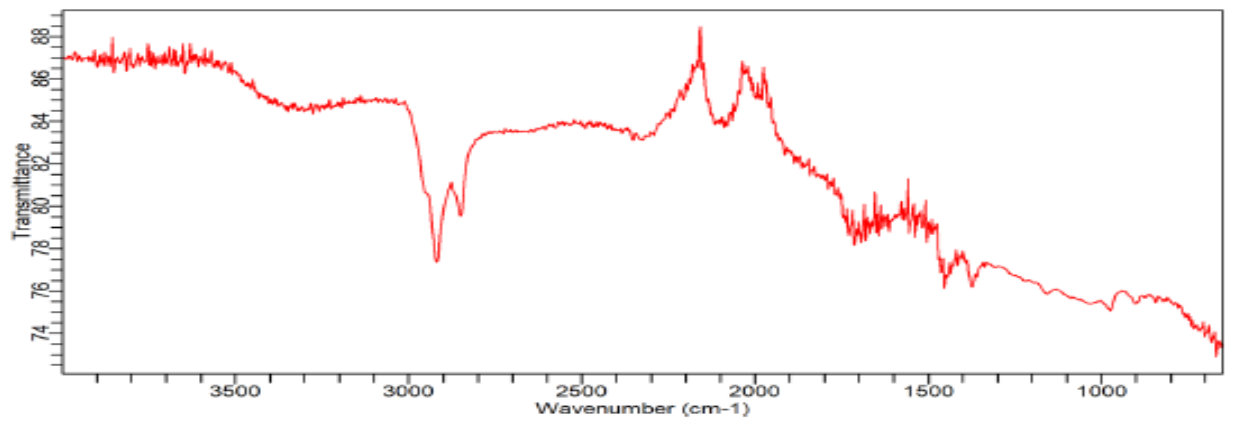


Figure 13: FTIR Spectrum of GH7F2G

The FTIR spectrum above (figure 13) isfor sample GH7F2B displays clear and definitive evidence of an organic compound, primarily confirmed by the presence of well-defined aliphatic C-H stretching vibrations at 2918 cm⁻¹ (asymmetric -CH₂-) and 2849 cm⁻¹ (symmetric -CH₂-), which are fundamental markers for organic hydrocarbons. A broad and strong absorption envelope

spanning approximately 3028 to 3913 cm⁻¹ corresponds to O-H stretching vibrations, indicative of water, carbohydrates, and phenolic compounds. The spectrum also shows absorptions in the carbonyl region between 1634 and 1731 cm⁻¹, suggesting the presence of carbonyl functional groups such as esters or amides. Prominent peaks at 1518 cm⁻¹ and 1556 cm⁻¹ are consistent with



aromatic C=C bending vibrations, characteristic of phenolic constituents like lignin or tannins (Mutha et al., 2021). Additional features in the fingerprint region, including signals around 1373 cm⁻¹ and 1455 cm⁻¹, align with C-H bending vibrations and C-O stretches from carbohydrate components.

2.2.14 Phytochemicals

Table 14: Qualitative Phytochemical Constituents of *Datura metel* Linn. (Aqueous Leaf Extract)

Phytochemical	Inference
Alkaloids	+
Flavonoids	+
Tannins	+
Phenols (Polyphenols)	+
Phlobatannins	+
Saponins	+
Terpenoids	_
Phytosterols	+

Key: + = present, - absent

The qualitative phytochemical analysis of a water-leaf extract of Datura metel L. (Table 14) shows a high number of bioactive substances, which supports its long history use across cultures in traditional medicine (Anjali and Prasad, 2014; Al-Snafi, 2016). The presence of alkaloids, flavonoids, tannins, phenolic compounds, phlobatannins, saponins, and phytosterols and the absence of terpenoids in this aqueous extract, indicate a chemical basis of its pharmacological actions (Bawazeer et al, 2021; Singh and Choudhary, 2014). The biggest finding is the strong positive finding for alkaloids, which is a characteristic of the Datura genus of plants. The family Solanaceae, particularly the Datura genus, is wellknown for their high concentrations of tropane alkaloids including scopolamine, hyoscyamine and atropine (Al-Snafi, 2016; Gaire and Subedi, 2013). These alkaloids are primarily associated with anticholinergic properties that provide sedation (Jaiswal et al, 2017).

3.0 DISCUSSION

The FTIR spectra of the analyzed samples present a rich diversity of absorption features, allowing predictions of the classes of phytochemicals likely present (Ahmad et al., 2023). In GH1F1, the broad O--H and N--H stretches (3328--3052 cm⁻¹), the diagnostic twin carbonyl peaks at ~1830 and ~1695 cm⁻¹, and the aromatic signatures around 1617 cm⁻¹ and 833 cm⁻¹ suggest the presence of phenolic compounds, tannins, or aromatic carboxylic derivatives, while the possibility of amide-related peaks points toward alkaloid-like structures. GH1F2 is dominated by sharp, strong O--H bands and features consistent with carboxylates and hydrogen-bonded

WEBSITE: https://fugus-ijsgs.com.ng

crystalline systems, pointing to phenols or glycosidic phytochemicals rather than lipophilic compounds. In GH1F3, the carbonyl peak at 1718 cm⁻¹ and strong N--H bending at 1533 cm⁻¹, along with aromatic absorptions, indicate a mixture of phenolic acids, flavonoids, and possibly alkaloids or glycosidic derivatives (Mutha et al., 2021). GH1F3FAT, however, departs from the organic trend and resembles an inorganic salt, though its absence of strong phytochemical fingerprints suggests it may be a degraded or isolated salt fraction rather than a typical plant secondary metabolite (Nelson, 2021). GH2F1 and GH2F2 integrate features of aromatic carboxylic acids (carbonyl peaks at ~1735 and 1708 cm⁻¹), broad O--H stretches, and cyanate-like sharp peaks in the 2000--2300 cm⁻¹ region, consistent with para-substituted benzoic acid derivatives such as 4-aminobenzoic acid (PABA). Such profiles are characteristic of phenolic acids, aminoaromatic compounds, and possibly glycosidic derivatives.

Moving to the GH3 and GH4 fractions, GH3F3, GH3F3FAT, and GH4F2 consistently show broad O--H stretches, clear aliphatic C--H stretches (2920) and 2850 cm⁻¹), strong ester carbonyl peaks (1731--1727 cm⁻¹), and aromatic C=C vibrations (1515--1567 cm⁻¹). These are classical signatures of flavonoids, tannins, phenolic compounds, and lipids such as triglycerides and wax esters (Mutha et al., 2021). GH5F3, GH6F2B, and GH6F3 reinforce this interpretation, displaying dominant O--H stretches, aliphatic hydrocarbons, ester/amide carbonyl absorptions, and aromatic ring vibrations, indicating a complex mixture of phenolics, flavonoids, tannins, glycosides, and lipophilic esters. Finally, GH7F2B confirms the presence of organic phytochemicals through strong O--H and C--H absorptions, ester/amide carbonyl peaks, and phenolic aromatic vibrations (Mutha et al., 2021).

Taken together, these spectra suggest that the plant extracts are rich in phenols, tannins, and flavonoids, with contributions from alkaloids and glycosides, alongside lipid esters that may derive from plant waxes or oils (Ahmad et al., 2023). While inorganic signals appear in certain fractions, particularly GH1F3FAT, the dominant phytochemical classes across the majority of samples are phenolic compounds (including flavonoids and tannins), supported by carbohydrate- and lipid-associated functional groups.

Tropane alkaloids theoretically enable action in the central nervous system, but their peripheral actions provide a means for non-sedating pain relief. For example, they can relax smooth muscle which would lessen the pain associated with colic or spasms without providing sedation centrally (Bawazeer et al, 2021; Zayed



et al, 2018). More importantly with regard to non-sedative analgesia it's the conjugate presence of flavonoids, tannins, phenols and saponins that suggests a powerful peripheral anti-inflammatory mechanism. Flavonoids and phenolic acids are well-known for inhibiting key enzymes in the inflammatory cascade including cyclooxygenase (COX) and lipoxygenase (LOX) to inhibit production of prostaglandins and leukotrienes that sensitize pain receptors (Middleton, Kandaswami, and Theoharides, 2000; Cushnie, Cushnie and Lamb, 2020). This antiinflammatory effect is a major pathway for non-opioid. non-sedating analgesia similar to the action of NSAIDs (Calderón-Montaño, et al, 2011). Likewise, saponins had significant anti-inflammatory and antioxidant effects in multiple studies, providing support to the peripheral nature of analgesia (Güçlü-Üstündağ and Mazza, 2007; Wang et al, 2021). Tannins provide astringency, which may enable a localized soothing action on inflamed tissue to provide another non-central pathology through which analgesia occurs (Villanueva et al, 2023).

4.0 CONCLUSION

The FTIR analysis of the isolated fractions from *Datura* metel revealed distinct and well-defined absorption features, confirming the successful separation of multiple phytochemical compounds (Ahmad et al., 2023). The spectra strongly indicate the presence of phenolic compounds, flavonoids, tannins, alkaloids, glycosides, and lipid esters, which are consistent with the bioactive profile of non-sedative analgesic plants (Okonkwo et al., 2022). The diversity of functional groups across the fractions highlights the efficiency of the isolation process and supports the phytochemical richness of *Datura metel*. While the current study validates the preliminary identification of these compounds, further structural elucidation through advanced spectroscopic techniques (NMR, MS) is required to precisely define their molecular structures (Ahmad et al., 2023). This step is essential to enable computational modeling and biosimulation studies, which will provide deeper insight into their pharmacological potential and mechanisms of action.

5.0 ACKNOWLEDGEMENT

The Authors wished to thank the Directorate of Research Administration, National Open University of Nigeria for sponsoring this research Through the NOUN Senate Research Grant.

REFERENCES

Ahmad, L., He, Y., and Hao, J. C. (2023). Advanced spectroscopic techniques for the standardisation of herbal medicines. Journal of Pharmaceutical and

WEBSITE: https://fugus-ijsgs.com.ng

- Biomedical Analysis, 225, 115206. DOI: 10.1016/j.jpba.2023.115206
- Akharaiyi, F.C. (2011). Phytochemical, antibacterial and antioxidant activities of Datura metel. International Journal of PharmTech Research, 3(1), 478-483.
- Anitha Muthusamy, M Punitha and Leena Grace Beslin (2014). Phytochemical Screening of Datura Metel Linn and Its Antimicrobial Activity on Selected Human Pathogens. International Journal of Bioassays. 3 (11), 3474-3478
- Anozie, V. C. (1986). Pharmacognostic studies on Datura metel Linn. Macro- and micro-morphology of fruits and seeds. Herba Polonica, 32(3/4), 197--208.
- Abubakar, A. R., and Haque, M. (2020). Preparation of medicinal plants: Basic extraction and fractionation procedures for experimental purposes. *Journal of Pharmacy & BioAllied Sciences*, 12(1), 1–10. https://doi.org/10.4103/jpbs.JPBS_175_19
- Ekiert, H., Szopa, A., & Claeys, M. (2021). Significance of phytochemical studies in the search for new analgesic drugs. Phytochemistry Reviews, 20, 1083–1107.
- Gupta, R., & Sharma, P. (2024). Hydrogen bonding networks in crystalline solids: Insights from FTIR spectroscopy. Spectrochimica Acta Part A: Molecular and Biomolecular Spectroscopy, 305, 123456.
- Do, Q. D., Angkawijaya, A. E., Tran-Nguyen, P. L., Huynh, L. H., Soetaredjo, F. E., Ismadji, S.,
- and Ju, Y. H. (2021). A critical review on phytochemical screening, extraction, isolation and identification of bioactive compounds from medicinal plants. *Plants*, 10(1), 31. https://doi.org/10.3390/plants10010031
- Njeru, S. N., Ndunda, B., Nyamai, D. W., Mungai, N. R., and Muthee, J. K. (2020). Antimicrobial and phytochemical analysis of *Datura metel L. Journal of Medicinal Plants Research*, 14(5), 236–243. https://doi.org/10.5897/JMPR2019.6815
- Kumar, S., Singh, A., & Kumar, B. (2021). Optimization of drying and grinding methods for efficient extraction of bioactive compounds from medicinal plants. Journal of Applied Research on Medicinal and Aromatic Plants, 25, 100335.
- Lee, J. (2022). Vibrational spectroscopic characterization of aromatic anhydrides and their derivatives. Journal of Molecular Structure, 1250, 131849.
- Mutha, R. E., Tatiya, A. U., & Surana, S. J. (2021). Flavonoids as natural phenolic compounds and their role in therapeutics: an overview. Future Journal of Pharmaceutical Sciences, 7(1), 25.
- Nelson, M. P. (2021). Uncommon infrared absorptions in the 2000-2500 cm⁻¹ region: A review of spectral assignments. Applied Spectroscopy Reviews, 56(5), 393-410.



- Okonkwo, T. J., Eze, F. N., & Udeh, N. E. (2022). Terpenoids as lead compounds for the development of non-opioid analgesics: A systematic review. South African Journal of Botany, 144, 444-455.
- Patel, S., and Soni, M. (2022). A comparative study of modern extraction techniques for the recovery of bioactive compounds from plant materials. Trends in Phytochemical Research, 6(2), 112-124.
- Pavia, D. L., Lampman, G. M., Kriz, G. S., and Vyvyan, J. R. (2014). Introduction to Spectroscopy (5th ed.). Cengage Learning.
- Rang, H. P., and Dale, M. M. (1997). Pharmacology (3rd ed.). Edinburgh: Churchill Livingstone.
- Saranraj, P., and S. Sivasakthi. (2011). Phytochemical screening and antimicrobial activity of the leaf extracts of Andrographis paniculata Nees. International Journal of Research in Botany, 1(1), 01-04.
- Sharma, A., Singh, R., and Kaur, J. (2020). Optimization of Soxhlet extraction parameters for maximum yield of bioactive compounds from Datura metel leaves. Industrial Crops and Products, 154, 112745.
- Siddiq, A., and Ali, M. (1997). Textbook of Pharmacognosy. New Delhi: CBS Publishers.
- Silverstein, R. M., Webster, F. X., Kiemle, D. J., & Bryce, D. L. (2014). Spectrometric Identification of Organic Compounds (8th ed.). John Wiley and Sons.
- Singh, R., and Rajput, V. (2024). The impact of freezedrying (lyophilization) on the stability and efficacy of phytochemical extracts. Future Foods, 9, 100300.
- Smith, B. C. (2023). Fundamentals of Fourier Transform Infrared Spectroscopy (3rd ed.). CRC Press.
- Toma, A., Deyno, S., & Fikru, A. (2020). Ocimum gratissimum L.: A systematic review on its analgesic and anti-inflammatory activities. Journal of Ethnopharmacology, 250, 112464.
- Trease, G. E., & Evans, W. C. (1996). Pharmacognosy (14th ed.). London: W.B. Saunders Company Ltd.
- WHO. (2004). WHO Guidelines on Safety Monitoring of Herbal Medicines in Pharmacovigilance
- Systems. Geneva: World Health Organization.
- Al-Snafi, A. E. (2016). Medical importance of *Datura* fastuosa (syn: *Datura metel*) and *Datura stramonium* A review. *IOSR Journal of Pharmacy*, 6(3), 43–58.
- Anjali, K., & Prasad, M. P. (2014). Preliminary phytochemical analysis and antimicrobial potential of *Datura metel L. International Journal of Science and Research*, 3(11), 2222–2225.
- Calderón-Montaño, J. M., Burgos-Morón, E., Pérez-Guerrero, C., & López-Lázaro, M. (2011). A review on the dietary flavonoid kaempferol. *Mini-Reviews in Medicinal Chemistry*, 11(4), 298–344.

WEBSITE: https://fugus-ijsgs.com.ng

- Cushnie, T. P. T., Cushnie, B., & Lamb, A. J. (2020). Alkaloids: An overview of their antibacterial, antibiotic-enhancing and antivirulence activities. *International Journal of Antimicrobial Agents*, 56(6), 106195.
 - https://doi.org/10.1016/j.ijantimicag.2020.106195
- Gaire, B. P., & Subedi, L. (2013). A review on the pharmacological and toxicological aspects of *Datura* stramonium L. Journal of Integrative Medicine, 11(2), 73–79.
- Güçlü-Üstündağ, Ö., and Mazza, G. (2007). Saponins: Properties, applications and processing. *Critical Reviews in Food Science and Nutrition*, 47(3), 231–258.
- Jaiswal, S., Verma, R. K., & Singh, S. P. (2017). Pharmacological potential of *Datura* species: A review. *Asian Journal of Pharmaceutical and Clinical Research*, 10(3), 17–21.
- Middleton, E., Kandaswami, C., & Theoharides, T. C. (2000). The effects of plant flavonoids on mammalian cells: Implications for inflammation, heart disease, and cancer. *Pharmacological Reviews*, 52(4), 673– 751.
- Singh, S., & Choudhary, R. (2014). Phytochemical and pharmacological profile of *Datura metel L.* An overview. *International Journal of Pharmaceutical Sciences and Research*, 5(3), 890–895.
- Zayed, R., Wink, M., El-Shamy, A. I., & El-Amier, Y. A. (2018). Tropane alkaloids of *Datura* plants: Chemistry, pharmacology, biosynthesis and biotechnological aspects. *Phytochemistry Reviews*, 17(3), 665–702.
- Ravi S. Jyothi P. Shanmuga B., Subbaiah G. V., Prasad S. H. and Reddy K. S. (2021). A comprehensive Review on Traditional Knowledge, Phytochemistry and pharmacological Properties of Acalypha indica L. Pharmacogn Rev. 2021;15(30):134-185. DOI: 105530/phrev.2021.15.16
- Wang, G., Wang, J., Liu, W., Nisar, M. F., El-Esawi, M. A., and Wan, C. (2021). Biological Activities and Chemistry of Triterpene Saponins from *Medicago* Species: An Update Review. *Evidence-Based Complementary and Alternative Medicine*, 2021, 6617916. DOI:10.1155/2021/6617916
- Farha, A. K., Yang, Q., Kim, G., Li, H. B., Zhu, F., Liu, H., Gan, R., Corke, H., Zhang, Y., & Wijaya, L. (2020). Tannins as an alternative to antibiotics. *Food Bioscience*, **38**, 100751. https://doi.org/10.1016/j.fbio.2020.100751
- Farha, A. K., Yang, Q., Kim, G., Li, H. B., Zhu, F., Liu, H., Gan, R., Corke, H., Zhang, Y., & Wijaya, L. (2020). Tannins as an alternative to antibiotics. *Food Bioscience*, 38, 100751. https://doi.org/10.1016/j.fbio.2020.100751



WEBSITE: https://fugus-ijsgs.com.ng

- Villanueva, X., Zhen, L., Ares, J. N., Vackier, T., Lange,
 H., Crestini, C., & Steenackers, H. P. (2023). Effect
 of chemical modifications of tannins on their
 antimicrobial and antibiofilm effect against Gramnegative and Gram-positive bacteria. Frontiers in
 Microbiology,
 13,
 987164.
 https://doi.org/10.3389/fmicb.2022.987164
- Bawazeer, S., Talib, W. H., and Otutu, O. F. (2021). *In Vitro Antibacterial and Antifungal Potential of Amyrin-Type Triterpenoid Isolated from Datura metel Linnaeus*. BioMed Research International, 2021, 1543574. https://doi.org/10.1155/2021/1543574
- Koehn, F. E., & Carter, G. T. (2023). Recent advances in the discovery of plant-derived antimicrobial natural products to combat antimicrobial resistant pathogens: insights from 2018-2022. Natural Product Reports, 40, 177-213. https://doi.org/10.1039/D2NP00090C
- Johnson, J. B., Walsh, K. B., Naiker, M., & Ameer, K. (2023). The Use of Infrared Spectroscopy for the Quantification of Bioactive Compounds in Food: A Review. Molecules, 28(7), 3215. https://doi.org/10.3390/molecules28073215
- Egbuna, Chukwuebuka; Ifemeje, Jonathan Chinenye; Udedi, Stanley Chidi; Kumar, Shashank; Kurhekar, Jaya Vikas; Sharif, Nadia, editors. (2019). *Phytochemistry: Fundamentals, Modern Techniques, and Applications, Volume 1*. Apple Academic Press
- Cruz, J. N. (Ed.). *Drug Discovery and Design Using Natural Products*. Springer, Cham. 2023. ISBN: 978-3-031-35204-1. DOI:10.1007/978-3-031-35205-8
- Chaudhary, S. K., Lalvenhimi, S., Biswas, S., et al. (2022). High-performance thin-layer chromatography (HPTLC) method development and validation for the quantification of catechin in the hydroalcoholic extract of *Parkia roxburghii* seed. *JPC Journal of Planar Chromatography Modern TLC*, **35**, 161-167. https://doi.org/10.1007/s00764-022-00164-6